

# Feedback-Enhanced MRI by Fixed-Point Dynamics and Nonlinear Spin-Locking

J. Furuyama<sup>1</sup>, and Y-Y. LIN<sup>1</sup>

<sup>1</sup>Chemistry & Biochemistry, UCLA, Los Angeles, CA, United States

## Introduction

Contrast in MRI and MR microscopy depends on the methodological ability to differentiate small differences in magnetic parameters across a sample plane. Contrast is limited, and consequently structural differentiation becomes increasingly difficult when magnetic properties do not vary significantly throughout the sample. We present a new approach that utilizes the unique spin dynamics in the presence of nonlinear feedback interactions, specifically the radiation damping feedback field. This approach yields novel contrast that is sensitive to small magnetic susceptibility variations. We demonstrate the unique spin dynamics within a sample due to the joint action of radiation damping feedback field and continuous-wave (CW) RF field in simulations, simple phantoms and *in vivo* guppy fish. Theoretical and experimental results show promise for use in biomedical study.

## Theory and Methods

Feedback based contrast enhancement utilizes the fields created by the sample itself to uniquely act back on the sample with the objective of amplifying the small magnetic differences across the sample, as shown in Fig. 1. To ensure the feedback field is unique to the sample itself, we can employ a local field  $\mathbf{B}(\mathbf{r},t)$  that is explicitly dependent on  $\mathbf{m}(\mathbf{r},t)$ , resulting in nonlinearity in the classical Bloch equations. At high field, the most prominent feedback field to manifest itself from the sample is the radiation damping feedback field, which is a result of a coupling between the average signal of the sample itself and the receiver coil as governed by the Lenz's Law. A constant perturbation to the sample via a low power CW at a frequency near the average precession frequency of the entire sample allows the magnetization,  $\mathbf{m}(\mathbf{r},t)$ , to continuously evolve in the presence of the radiation damping feedback field. Evolution of the magnetization under the specific MR parameters in the Bloch equations leads to small variations within the sample leading to  $\mathbf{m}(\mathbf{r},t_0+\Delta t)$ , which is immediately reflected in  $\mathbf{B}(\mathbf{r},t) = \mathbf{B}(\mathbf{m}(\mathbf{r},t_0+\Delta t))$  and subsequently acts back on the sample. Consequently, any subsequent evolution of the magnetization is characteristic to the sample itself because the local field is dependent on the magnetization of the sample.

Phantom samples were created using a 5% acetone solution in water to create a slight susceptibility variation from that of pure water. Micro-imaging experiments were performed *in vivo* on guppy fish. Images were acquired on a 600MHz spectrometer, using an MR micro-imaging probe with 5-mm saddle coil optimized for proton sensitivity.

## Results

Figure 2 shows the simulated evolution of magnetization for a sample with two frequency components. Application of a CW at a frequency between these two components effectively pushes the orientation of both components to opposite poles of a unit magnetization sphere (the Bloch sphere). This fixed-point phenomenon requires the presence of radiation damping because contrast evolution resulting strictly from precession only will eventually converge back on itself. Allowing radiation damping to feedback into the sample diverges the orientation of the different magnetization vectors, resulting in a remarkable contrast mechanism. Experimental images shown in Fig. 3 were obtained on a simple phantom to verify the dynamics predicted by the theoretical calculation. It can be seen from the image that the 5% acetone solutions within the capillaries have a positive magnetization with respect to the reference phase, where the pure water on the outside has a negative magnetization, as would be expected from theory.

Comparative experimental *in vivo* images of guppy fish are shown in Fig. 4. All images were taken at the same axial slice for methodological comparison. The proton density image (4A) yields little contrast and little-to-no information regarding magnetic susceptibility of particular tissues. The  $T_2^*$  image (4B) gives insight into microscopic inhomogeneity on the subpixel level, yet falls short of improved contrast. Susceptibility weighted image (SWI, 4C) obtained from two  $T_2^*$  images taken at different TE times gives susceptibility distribution in the tissue. Figure 4D shows the same slice acquired with a low power CW in the presence of radiation damping. It can be seen that the imaging contrast resembles the SWI but with much higher image clarity.

## Discussion and Conclusions

The joint action of the radiation damping feedback field and CW RF field enhances the contrast originated from magnetic susceptibility variations. These variations correlate more directly with physiological conditions such as water contents and oxygenation level (i.e., relative concentrations of oxyhemoglobin, deoxyhemoglobin, and methemoglobin) and thus can be used to differentiate tissue types including tumors and lesions. To adapt feedback-enhanced contrast for *in vivo* imaging at lower fields, the radiation damping field can be actively reinforced through electronic feedback to the induced current. Such active-feedback enhanced images will also be presented.

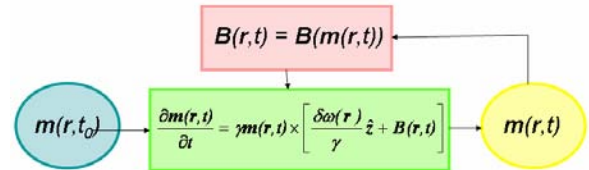


Fig. 1. Flowchart of feedback-based contrast enhancement

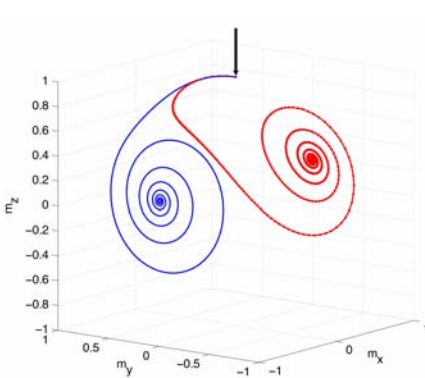


Fig. 2. Trajectories of magnetization evolution in a 2-frequency components system

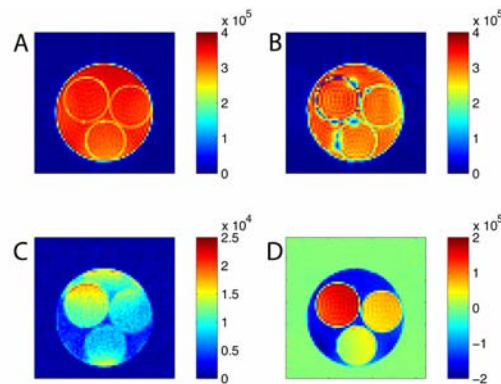


Fig. 3. Comparative experimental images of a simple phantom containing 5% acetone (inside capillaries) and water. (A) SD image; (B) T1 image; (C) T2\* image; (D) this new method

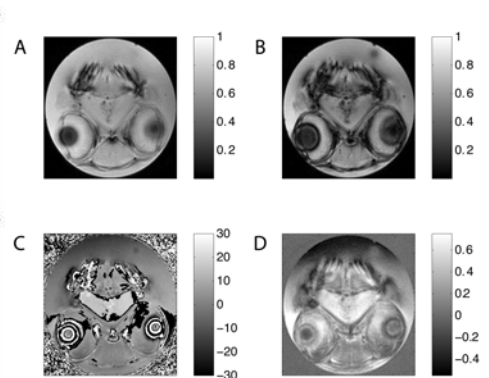


Fig. 4. Comparative experimental *in vivo* images of guppy fish. (A) SD image; (B) T2\* image; (C) SWI image; (D) this new method